

# Topology-Preserving $\lambda_2$ -based Vortex Core Line Detection for Flow Visualization

T. Schafhitzel<sup>1</sup> J. E. Vollrath<sup>2</sup> J.P. Gois<sup>3</sup> D. Weiskopf<sup>2</sup> A. Castelo<sup>3</sup> T. Ertl<sup>1</sup>

<sup>1</sup>Institute of Visualization and Interactive Systems, Universität Stuttgart, Germany

<sup>2</sup>VISUS, Universität Stuttgart, Germany

<sup>3</sup>Instituto de Ciências Matemáticas e de Computação, USP, Brazil

---

## Abstract

We propose a novel vortex core line extraction method based on the  $\lambda_2$  vortex region criterion in order to improve the detection of vortex features for 3D flow visualization. The core line is defined as a curve that connects  $\lambda_2$  minima restricted to planes that are perpendicular to the core line. The basic algorithm consists of the following stages: (1)  $\lambda_2$  field construction and isosurface extraction; (2) computation of the curve skeleton of the  $\lambda_2$  isosurface to build an initial prediction for the core line; (3) correction of the locations of the prediction by searching for  $\lambda_2$  minima on planes perpendicular to the core line. In particular, we consider the topology of the vortex core lines, guaranteeing the same topology as the initial curve skeleton. Furthermore, we propose a geometry-guided definition of vortex bifurcation, which represents the split of one core line into two parts. Finally, we introduce a user-guided approach in order to narrow down vortical regions taking into account the graph of  $\lambda_2$  along the computed vortex core line. We demonstrate the effectiveness of our method by comparing our results to previous core line detection methods with both simulated and experimental data; in particular, we show robustness of our method for noise-affected data.

Categories and Subject Descriptors (according to ACM CCS): CCScatI.3.3Computer GraphicsPicture/Image Generation J.2 [Physical Sciences and Engineering]:

---

## 1. Introduction

One of the open challenges for flow visualization is the appropriate display of 3D flow, in particular, for unsteady and intricate flow. Immediate, direct visualization of such input data leads to cluttered, hardly comprehensible images. Therefore, feature extraction is instrumental for appropriate visualization because it removes unnecessary parts of the data set to allow the user to focus on important elements. This paper focuses on vortex detection and visualization because vortices represent most important features for many applications and they transport most of the energy in vortical flow, strongly affecting flow evolution over time. A fundamental issue is the lack of a unique mathematical or physical definition of a vortex. As detailed in Section 2, the literature provides a range of different vortex criteria and corresponding detection algorithms, with respective advantages and disadvantages. Adopting the taxonomy of Jiang et al. [JMT05], vortex-detection algorithms can be classified

according to three categories: (1) whether they detect 3D vortex regions or 1D vortex core lines; (2) whether they are Galilean invariant or not; (3) whether they are local or global (i.e., whether they require operations only in the local neighborhood of a grid cell or not). Generally, 3D region-based methods are easier to implement and more efficient, whereas 1D line-based methods have to determine vortex core lines accurately and might be more sensitive toward noise. On the other hand, a line-based visual representation is more concise than a 3D region and, thus, is preferable from a visualization point of view. With respect to the second category, we only consider Galilean invariant criteria because they are immediately applicable to moving vortices in unsteady flows. Finally, local methods tend to be easily computed by local operations whereas global methods typically are more costly. However, since vortices are global features, a global method tends to be more accurate.

The basic idea of this paper is to enrich the  $\lambda_2$  crite-

rion [JH95], which is a region-based, Galilean invariant, and local vortex criterion, such that it allows us to construct 1D vortex core lines. In this way,  $\lambda_2$  serves as basis for global, line-oriented vortex core detection. We have chosen  $\lambda_2$  because it is considered by many fluid-mechanics engineers to be most effective and reliable for detecting vortices in incompressible flows (except for very special cases with strong axial stretching [WXY05]). Our algorithm consists of the following stages: First, the scalar field of  $\lambda_2$  is constructed and the corresponding isosurface is extracted. Second, the isosurfaces are reduced to 1D representations by skeletonization. These skeletons serve as initial prediction of the core lines. Third, the locations of the skeleton prediction are corrected by searching for  $\lambda_2$  minima on planes perpendicular to the core line.

The main contributions of this paper are: (1) We propose a vortex core line detection method that is based on skeletonization and that makes use of a local direct search for core line points. (2) A geometric model for vortex bifurcations, where two vortex cores merge, is introduced. (3) Vortex breaks are supported by the automatic computation of  $\lambda_2$  isovalues at which vortex regions separate.

Our approach is generic in the sense that it would work with scalar fields other than  $\lambda_2$ , as long as vortex core lines can be found by local extrema on planes of that scalar field.  $\lambda_2$ -based vortex core line detection offers several benefits. First, it combines the simplicity and conciseness of a vortex core line with excellent detection quality of  $\lambda_2$ . Second, the core lines are guaranteed to reflect the connectedness of the underlying  $\lambda_2$  isosurface: there is the same number of connected components of core lines and isosurfaces. Furthermore, we even guarantee that the core line has the same topology as the  $\lambda_2$  isosurface skeleton. Third, the core line detection is less sensitive to noise and other fluctuations in data values, as demonstrated by the evaluation with noisy experimental data sets. In summary, our approach leads to a compact and reliable presentation of the vortical structure of flow.

## 2. Previous Work

Feature-based flow visualization in general and vortex detection in particular are well-investigated research fields, an overview of which can be found in the survey articles [JH95, PVH\*03]. A popular region-based, local vortex criterion is the  $\lambda_2$  method by Jeong and Hussain [JH95], which is based on the evaluation of the Jacobian of the vector field by matrix decomposition and eigenvalue computation. Related earlier methods based on the Jacobian include the  $Q$  criterion [HWM88] and the  $\Delta$  criterion [CPC90, Dal83]. Other typical criteria use helicity or magnitude of vorticity. These criteria are the basis for a variety of vortex core extraction algorithms, including [BS95, BP02, PR99, SB94, SWH05, SH95, TSW\*05]. The parallel-vectors approach [PR99] generalizes several prior extraction approaches, including [SH95].

Adopting the concept of feature flow fields [TS03], the parallel-vectors operator can be used to trace ridge and valley lines of local criteria like  $\lambda_2$  from local extremum points [SWH05]. This idea can be extended to track core lines over time [TSW\*05]. Recently, Weinkauff et al. [WSTH07] have extended this class of algorithms by proposing the coplanar-vectors operator, which is applied to the extraction of cores of swirling particle motion in transient flows. The parallel-vectors/feature flow field approach and our method share the same basic goal: extracting minimal lines of  $\lambda_2$ . However, our method avoids the higher-order derivatives of the  $\lambda_2$  scalar field that are required by the parallel-vectors/feature flow field approach. Furthermore, we propose a robust core line search algorithm that guarantees that only one connected core line component is extracted for one connected  $\lambda_2$  region. In contrast, higher-order derivatives of  $\lambda_2$  are sensitive toward fluctuations of the vector field, they require a careful filtering or reconstruction of the input, and they might lead to a large number of unwanted core lines (i.e., false positives).

Our method is similar to those of Banks and Singer [BS95, SB94] and Stegmaier et al. [SRE05] in the sense that all three methods apply a predictor-corrector approach, with direct search [HJ61] for extremum values on 2D planes in order to correct the predicted core line locations. Banks and Singer [BS95, SB94] search for pressure minima and Stegmaier et al. [SRE05] search for  $\lambda_2$  minima. Both previous approaches use vorticity in order to predict subsequent positions on the core line. We also use  $\lambda_2$  minima for the correction step, but the prediction part utilizes the initial skeleton of the  $\lambda_2$  isosurface because vorticity might not lead to a good prediction. More importantly, Stegmaier et al. [SRE05] only consider single core lines, without any vortex bifurcations or vortex break.

Skeletonization is the process of extracting a medial surface or medial axis, the curve skeleton, from a geometric object. In particular, curve skeletons offer a condensed 1D representation of the topology of an object and are thus used in a variety of applications, ranging from animation to virtual endoscopy. A comprehensive survey is given by Cornea and Min [CM07].

## 3. Theoretical Basis

This section briefly reviews the region-based  $\lambda_2$  criterion [JH95], which serves as basis for our vortex core line detection. Then, the  $\lambda_2$  criterion is related to core line detection in the form of valley lines.

### 3.1. $\lambda_2$ Vortex Criterion

The  $\lambda_2$  vortex criterion bases on the assumption of low pressure inside vortical structures. It improves the accuracy of detecting vortical regions by disregarding components that

might lead to inaccuracies between the existence of a pressure minimum and the existence of a vortex. Galilean invariance is retained, i.e., the  $\lambda_2$  method delivers identical solutions even when a constant vector is added to the vector field. This is quite important when different reference frames are used. Actually, the  $\lambda_2$  method bases on the symmetric part of the acceleration gradient of the Navier-Stokes equations and leads to

$$\frac{DS_{ij}}{Dt} - \nu S_{ij,kk} + \Omega_{ik}\Omega_{kj} + S_{ik}S_{kj} = -\frac{1}{\rho}p_{,ij}, \quad (1)$$

where  $\nu$  denotes the viscosity,  $p_{,ij}$  the Hessian of the pressure, and  $S$  and  $\Omega$  the symmetric and antisymmetric parts of the velocity gradient tensor, respectively. The first two terms of the left-hand side are neglected; the first stands for unsteady irrotational straining, which can create a pressure minimum without a vortical or swirling motion. The second represents viscous effects, which might eliminate a pressure minimum inside a vortical region. This leads to a new matrix  $M = S^2 + \Omega^2$ , i.e., the addition of the quadratic strain tensor and the quadratic rotation tensor, which represents the reformulated Hessian of pressure. Since  $M$  is real and symmetric, it has exactly three real eigenvalues, which can be sorted according to  $\lambda_1 \geq \lambda_2 \geq \lambda_3$ . The value for the  $\lambda_2$  vortex criterion is identical to the above eigenvalue  $\lambda_2$ . According to Jeong and Hussain [JH95], a vortical region is identified if  $M$  has two negative eigenvalues, i.e.  $\lambda_2 < 0$ , and is covered by  $\lambda_2$  isosurfaces with isovalue 0. Decreasing negative  $\lambda_2$  values correspond to increasing vortex strength. Therefore, vortices are often extracted by isovalues less than 0 in order to remove weak vortices.

### 3.2. Vortex Core Lines

The motivation for defining core lines is based on the idea of minimum lines of  $\lambda_2$  because large negative values of  $\lambda_2$  denote strong vortex behavior. A non-degenerate  $\lambda_2$  would lead to isolated local minima of  $\lambda_2$ , i.e., to 0D instead of 1D features. In general, a sufficient condition for a local minimum of a 3D scalar function  $f(\mathbf{x})$  is a vanishing gradient,  $\nabla f(\mathbf{x}) = 0$ , and three positive eigenvalues of the Hessian  $\mathcal{H}f$  containing the second order partial derivatives of  $f(\mathbf{x})$ , which is a real, symmetric matrix.

The generalization of minimum points to minimum lines, also called valley lines, requires us to relax these conditions. Since we want to allow for a variation of the gradient along the valley line, we require a point on it to be only a minimum on a plane orthogonal to its tangent vector. In [MK97, PR99] it has been shown that valley lines are required to have the minimal slope  $|\nabla f(\mathbf{x})|$  of all points of the same elevation  $f(\mathbf{x})$ . This means that  $|\nabla f(\mathbf{x})|$  needs to be a minimum in direction of smallest change of  $f$ , which can be approximated by a plane orthogonal to  $\nabla f$ . In detail, that requires the gradient to be an eigenvector of the Hessian  $\mathcal{H}f$ . If the eigenvalues of  $\mathcal{H}f$  are defined in a consecutive order  $\eta_0 \geq \eta_1 \geq \eta_2$  and  $\mathbf{e}_i$  denotes the respective eigenvectors, then a point lies

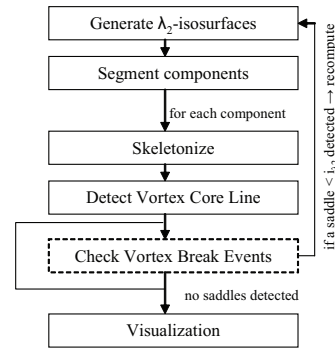


**Figure 1:** Program flow for the computation of vortex core lines.

on a valley line if  $\eta_1 > 0$  and  $\mathbf{e}_2 = \text{const} \cdot \nabla f$  are fulfilled. That implies that  $f(\mathbf{x})$  is a minimum on the plane orthogonal to the valley line, but not necessarily on the valley line itself.

The problem of finding valley lines was reformulated by Peikert et al. [PR99] by using the parallel-vectors operator. According to their definition, an extremum line of  $f$  is defined by  $\nabla f \parallel (\mathcal{H}f)\nabla f$ , which claims, similar to the description above,  $\nabla f$  to be an eigenvector of the Hessian  $\mathcal{H}f$ . Also the definition of a valley line is similar: let  $\mathbf{e}_2$  be aligned with  $\nabla f$ , then  $\eta_0 > \eta_2$  and  $\eta_1 > \eta_2$  have to be fulfilled. A similar formulation was given by Haralick [Har83] and Eberly [Ebe96].

In this paper, we follow a search approach on the planes perpendicular to the vortex core line. However, the vortex core yet needs to be determined and, thus, the aforementioned perpendicular direction is not yet known. It is guaranteed that the deflection of the eigenvectors of  $\mathcal{H}$  from those at the point  $\mathbf{x}_0$  is rather small for any point within a close distance. In other words, a point on the vortex core line can be identified as a minimum on a plane  $P$  through a predicted position  $\mathbf{x}'$  if the distance  $|\mathbf{x}' - \mathbf{x}_0|$  is small enough and the orientation of the plane differs not too much from the plane spanned by  $\mathbf{e}_0$  and  $\mathbf{e}_1$  at  $\mathbf{x}_0$ . We implement this search idea by following a predictor-corrector scheme. In the first stage, a position nearby the vortex core line is determined. Then, in order to find the next point on the vortex core line (i.e., the corrected position), a plane is created at the predicted position perpendicular to the tangent vector of the curve skeleton of the  $\lambda_2$  isosurface.

### 4. Vortex Core Line Detection

This section describes the individual steps of our algorithm—in the order of their appearance in the program flow (Figure 1).

#### 4.1. Isosurface Generation, Segmentation, and Skeletonization

The algorithm starts by computing the  $\lambda_2$  field and its corresponding isosurface. The isovalue  $\lambda_2 = 0$  yields the representation of all vortical regions, enclosed by the isosurface [JH95]. To treat vortical regions individually, segmentation is applied to the  $\lambda_2$  isosurface: individual vortical regions are identified by searching the isosurface for disjoint components. By confining the skeletonization process to each component individually we obtain a curve skeleton for each vortical region. In the remainder of this paper we refer to the curve skeleton of a vortical region as *isoskeleton*.

#### 4.2. Searching the Core Line

According to Section 3.2, the vortex core line is defined as a connected set of plane-restricted local  $\lambda_2$  minima, where the search plane is perpendicular to the tangent vector of the core line. However, the core line and its tangent vector are yet unknown during the detection phase. This makes it necessary to find an appropriate estimate of the core line. We approximate the tangent vector of the vortex core line by the tangent vector of the isoskeleton. Since the vortex core line is generally defined as a one-parameter, 3D space curve that serves as a geometrical, and often dynamical, simplification of a vortex, the isoskeleton provides a good initial approximation of the vortex core line.

In contrast to the vorticity vector used by Stegmaier et al. [SRE05] or the second derivative of  $\lambda_2$  used by the parallel-vectors operator [PR99], the isoskeleton has been shown to be less sensitive to the presence of noise in the data, as discussed in Section 6. Furthermore, the isoskeleton provides information about the possibly non-trivial topology of the vortex core line: vortex bifurcation is an example of the split of a vortex core line into two lines, which is supported by the isoskeleton description (see Section 4.3).

Algorithm 1 shows how the isoskeleton curve  $\Gamma(s)$  is used to find a single-component vortex core line. Metaphorically speaking, we view the isoskeleton as a handrail guiding the core line search algorithm. Starting at the first point of the isoskeleton,  $\Gamma(0)$ , we step along the isoskeleton until the endpoint,  $\Gamma(\text{numPoints} - 1)$ , where *numPoints* describes the number of points of the polygonal representation of  $\Gamma$ . At the first sample point on the isoskeleton, the plane perpendicular to the isoskeleton tangent vector  $d\Gamma/ds$  is created to search the plane-restricted  $\lambda_2$  minimum. The search region is restricted to the part of the plane contained within the  $\lambda_2$  isosurface. Using the minimum found as first point of the vortex core line,  $\text{pos}[0]$ , the algorithm loops over the remaining points  $\Gamma(i)$  of the isoskeleton to construct the rest of the vortex core line. The tangential vector of the isoskeleton is used to predict the position of the next minimum. The predicted position *pred* is computed by moving from the current point

$\text{pos}[i - 1]$  on the vortex core line along the tangent direction  $d\Gamma/ds$  at location  $(i - 1)$ . The idea is to move piecewise parallel to the isoskeleton, where the stepsize is defined by the distance between the sample points on the isoskeleton. Once we have found the predicted position *pred*, again a plane is created, orthogonal to the tangent vector of the current sample on the isoskeleton. The  $\lambda_2$  minimum on the plane defines the corrected position  $\text{pos}[i]$  of the next sample of the vortex core line. Subsequently, the algorithm loops over all sample points on the isoskeleton. Once the endpoint of the isoskeleton is reached, the algorithm terminates. The result is a number of plane-restricted  $\lambda_2$  minima connected according to the topology of the isoskeleton. Note that the computed vortex core line is independent of the starting point of the algorithm ( $\Gamma(0)$  or  $\Gamma(\text{numPoints} - 1)$ ) because the orientations of the search planes are always given by  $d\Gamma/ds$ , which is independent of the order of curve traversal when computed through central differences.

One problem is the issue of different parameterizations of the isoskeleton and the vortex core line curves because one curve might propagate faster than the other, particularly in areas of high curvature. As a consequence, sample points on the isoskeleton might be wrongly related to points on the vortex core line. This problem is overcome by adaptively choosing the sampling distance along the two curves, implying an intrinsic reparameterization of the curves. In detail, for each new point on the vortex core line, the distance to its corresponding sample point on the isoskeleton is computed. If the distance is larger than a threshold, e.g., one cell, the position on the core line is recomputed using the half step size for integration. In the case the distance became larger after correction, the core line seems to grow more slowly than the isoskeleton, and therefore, the initial step size is doubled. This process is repeated until the distance between the core line and the skeleton is smaller than the given threshold. Figure 2 illustrates an example of the problem and its solution by reparameterization.

---

#### Algorithm 1 Detection of vortex core lines.

---

```

void computeVortexCoreLine(IsoSkeleton  $\Gamma$ )
{
  // Compute the first position on the vortex core line
  create plane  $P \perp \frac{d\Gamma}{ds}(0)$  at  $\Gamma(0)$ ;
   $\text{pos}[0] = \min(\lambda_2)$  on  $P$ ;
   $\text{numPoints} = \text{NumOfDiscreteSamplePoints}(\Gamma)$ ;
  // Loop along the isoskeleton
  for  $i=1$  to  $\text{numPoints}-1$ 
    // Predict the new position
     $\text{pred} = \text{pos}[i-1] + \text{stepsize} * \frac{d\Gamma}{ds}(i-1)$ ;
    // Create a plane perpendicular to the isoskeleton tangent vector:
    create plane  $P \perp \frac{d\Gamma}{ds}(i)$  at  $\text{pred}$ ;
    // Correct the predicted position
     $\text{pos}[i] = \min(\lambda_2)$  on  $P$ ;
  endfor
}

```

---

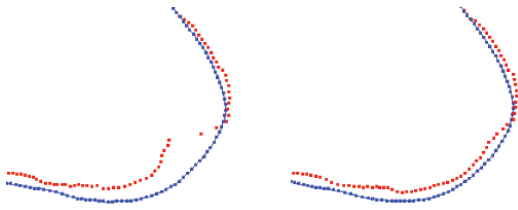


**Figure 2:** Parameterization issues: the red curve of the vortex core line grows faster than the blue curve of the isoskeleton (left). Therefore, the tangent vector for generating the search plane becomes corrupted. This problem is addressed by reparametrization of the vortex core line (right).

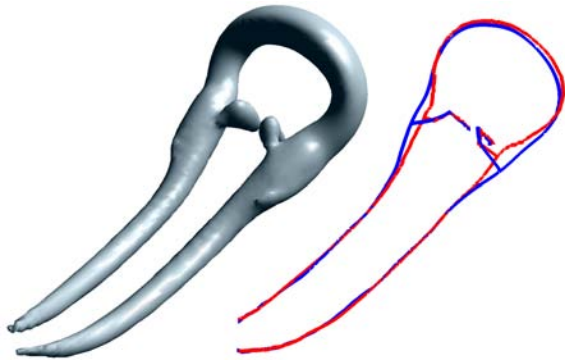


**Figure 3:** Isosurface (left) and core of a hairpin vortex in a transitional flow (right); both arms are growing temporally and are connected with the existing vortex structure. The vortex core line is colored in red and the isoskeleton in blue.

### 4.3. Vortex Core Line Splits

We define a *bifurcation* point as a point where a vortex core line splits into two parts (see Figure 3). A bifurcation is often the result of a temporal change of topology, e.g., due to *vortex reconnection*, which can be ascribed to a merge of two vortices rotating in opposite directions. Kida et al. [KT94] defined three types of reconnections: the vortex reconnection, the scalar reconnection, and the vorticity reconnection. While the vortex and scalar reconnection depend on isosurfaces of vorticity and any scalar quantity, respectively, the vorticity reconnection treats the topological changes of vorticity lines. Although it is known that in regions of vortex reconnection the closest vorticity lines are canceled by viscous diffusion [KT94], it was shown that the assumption of vanishing vorticity is only valid in 2D, not in 3D [YOH\*90]. The bifurcation of a vortex core line can also be ascribed to the generation of new vortices, e.g. in terms of an autogeneration process [Adr07]. Here, a so-called *feeder vortex* [BS95] might be generated, i.e., a vortex core line that enters an existing vortex structure to spiral towards its center.

However, to the authors' knowledge, there exists no formal definition of the bifurcations that might result from the previous discussion. To overcome this deficit, we model bi-

furcations by a geometric, skeleton-based approach: we propose that the vortex core line has the same topology as the isoskeleton of the  $\lambda_2$  isosurface enclosing a vortical region. We assume bifurcation of the vortex core line in regions where the isoskeleton has a bifurcation, i.e., as a result of scalar reconnection with respect to  $\lambda_2$ .

In Algorithm 2, we introduce a treatment of bifurcation points on the isoskeleton and the connecting isoskeleton segments, respectively. Now, Algorithm 1 is applied to individual segments and *unsafe regions* near bifurcations (i.e. where local  $\lambda_2$  minima might be shared by two or more segments, or regions where the spatial boundaries of the  $\lambda_2$  minimum search are not defined clearly) are treated in the following way: the search for plane-restricted  $\lambda_2$  minima is always performed in direction toward the bifurcation, starting from a remote *safe region*. Two types of segments are considered (Figure 4): a segment that either starts or ends at a bifurcation, and a segment that both starts and ends at a bifurcation. In the first case, the isoskeleton is traversed starting at the non-bifurcation point by adapting the order of the isoskeleton's sample points (function *sortSegment*( $\Gamma$ )). In the second case, the traversal is started in the middle of the segment in both directions (function *splitSegment*( $\Gamma$ )).

Unsafe regions are detected by testing the vortex core lines for discontinuities. Similar to previous predictor-corrector approaches [BS95, SRE05], we identify discontinuities by checking for a large Euclidean distance between the predicted and the corrected  $\lambda_2$  minima. If a discontinuity is detected, adaptive search—with reduced stepsize along the isoskeleton—is employed to come as close as possible to the unsafe region by reliably computed  $\lambda_2$  minimum points. Finally, the missing piece between two adjacent vortex core

---

#### Algorithm 2 Extended algorithm for vortex bifurcations.

---

```

void computeAllSegments(IsoSkeleton  $\Theta$ )
{
  numSegments = getNumberOfSegments( $\Theta$ );
  // Loop over all segments
  for j=0 to numSegments-1
    // Get the segment and its type
     $\Gamma$  = GetCurrentSegment( $\Theta$ , j);
    type = getSegmentType( $\Gamma$ );
    if(type == end-bif) // endpoint-bifurcation
      sortSegment( $\Gamma$ );
      computeVortexCoreLine( $\Gamma$ );
    else // bifurcation-bifurcation
      splitSegment( $\Gamma$ ,  $\Gamma_L$ ,  $\Gamma_R$ );
      sortSegment( $\Gamma_L$ );
      computeVortexCoreLine( $\Gamma_L$ );
      sortSegment( $\Gamma_R$ );
      computeVortexCoreLine( $\Gamma_R$ );
    // connect with segments sharing the same bifurcation points
    connectCoreLineSegments();
  endfor
}

```

---

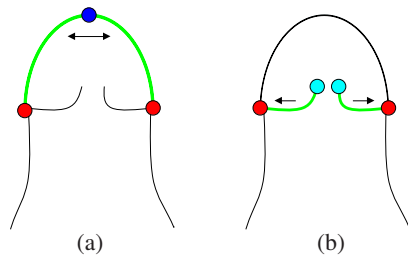


**Figure 4:** Connection types in an isoskeleton: connection of two red bifurcation points – by splitting the connecting segment and starting the search for local  $\lambda_2$  minima at the blue point it is assured that the search propagates toward the bifurcations (a); connection of cyan endpoints and red bifurcation points (b).

lines is filled by directly connecting the closest known  $\lambda_2$  minimum points (see function `connectCoreLineSegments()` in Algorithm 2). In our experience, the size of the missing piece depends largely on the resolution of the vector field and does typically not exceed one cell (mostly, it is much smaller). Due to the connection step, this method only delivers a topology preserving approximation of the bifurcations.

## 5. Semi-Automatic $\lambda_2$ -Isovalue Determination

In Jeong et al. [JH95] vortical regions are defined as spatial areas where  $\lambda_2 < 0$ . However, in practice, the condition of  $\lambda_2 < 0$  is rather insufficient because of its dependency on the accuracy of the  $\lambda_2$  values. The problem of potential inaccuracies is not easy to solve, regardless of they are caused due to a resampling process, i.e. by interpolating the data, or noise which mostly occurs in experimental data. Engineers usually overcome this problem by manually determining an appropriate  $\lambda_2$  isovalue. Considering the computation of vortex core lines, there are two issues to solve: on the one hand, the  $\lambda_2$  isovalue has to be chosen very small (i.e., large negative) to emphasize the vortical structures, and on the other hand, the  $\lambda_2$  isovalue should not be chosen too small because it would reduce the length of the detected vortex core lines, caused by shrinking isosurfaces when  $\lambda_2 \rightarrow -\infty$ . This makes it desirable to compute an optimal  $\lambda_2$  isovalue for each vortical region which is small enough to uncover all the individual vortex structures, but also only as small as necessary in order to prevent the vortex core lines to be shortened unnecessarily.

In this section we propose an algorithm for determining an appropriate  $\lambda_2$  isovalue. Since the desired visualization strongly depends on the user's experience, the proposed method works in a semi-automatic manner where the user's influence is given by a decay offset in terms of a parameter  $\epsilon$  (i.e., a window of  $\lambda_2$  values). The result of this method should be a number of vortex structures, each holding its individual optimal  $\lambda_2$  isovalue.

Typically, decreasing values of  $\lambda_2$  produce a hierarchy of nested isosurfaces with changing topology (and thus with changing vortex cores), akin to the contour tree [vKvOB\*97]. These changes of topology take place at the position of critical points contained in the interior of the initially computed isosurface. In particular, a break of an isosurface takes place at the positions of local  $\lambda_2$  maxima on the vortex core line, which we call a vortex break. Since all points are supposed to be minima on a plane perpendicular to the vortex core line, these curve related maxima can be considered as critical points, particularly as saddles in 3D. Therefore, saddle points may lead to vortex break events when the isovalue falls below the saddle's  $\lambda_2$  value. In contrast, if there is no saddle on the core line, the core line is guaranteed not to break.

We reduce the possible set of vortex break events by applying the following criterion to the saddle points:  $|\lambda_2(\mathbf{x}) - i_{\lambda_2}| < \epsilon$ , where  $\epsilon$  is the global user defined decay offset which is given as a percentaged value of the global  $\lambda_2$  minimum,  $i_{\lambda_2}$  the current isovalue ( $\lambda_2 = 0$  at beginning) and  $\mathbf{x}$  the position of a critical point, which is supposed to be a saddle in 3D and a global  $\lambda_2$  maximum on the respective vortex core line. If such a saddle is found, the isosurface is recomputed with  $\lambda_2(\mathbf{x})$ . Since we assume the critical points of the  $\lambda_2$  field and thus also the saddles to be isolated, the part of the isosurface within the vortical region under consideration will decompose into two disjoint components at the new isovalue. For these components, the entire process of vortex core line detection, including the aforementioned vortex break detection, is performed in a recursive manner (see Figure 1). The recursive way of operation guarantees the core detection to operate locally on vortical regions, traversing the hierarchy of nested components of the  $\lambda_2$  isosurfaces for different isovalues from top to bottom. In addition, it allows for the detection of different vortex cores to be based on different values of  $\lambda_2$ . It furthermore offers control to the user via the parameter  $\epsilon$ .

## 6. Implementation Details, Results, and Discussion

For  $\lambda_2$  isosurface extraction we make use of a marching cubes implementation with topological guarantees [LLVT03]. This implementation is beneficial because individual vortical regions are identified based on the topology of the isosurface geometry, as described in the following paragraph. In order to process vortices individually, a segmentation of the  $\lambda_2$  isosurface into disjoint components is carried out. Given the output of the isosurfacing algorithm as a triangle soup encoded in indexed triangle and vertex lists, such components are identified by using the instance of a shared vertex between triangles as a grouping criterion.

For our purposes the isoskeleton, which guides the core line extraction algorithm, is required to be a smooth ( $C^1$  continuous) curve. The skeletonization algorithm proposed by Cornea et al. [CSYB05] has the property of producing



**Figure 5:** Our approach faithfully extracts a vortex core line that consists of several connected components (left). The approach by Stegmaier et al. extracts components of the vortex core line that are equivalent to our results but remain unconnected (middle). The  $\lambda_2$ -based parallel-vectors approach extracts unconnected points on the vortex core line; several outliers are present as well as sections where no core line points were detected (right).



**Figure 6:** Semi-automatic isovalue determination: original vortical region (left); decomposition with color coding by isovalue (middle); the respective vortex core lines (right).

smooth curves and was thus the method of choice. Clearly, not all skeletonization algorithms produce smooth curves. Since any isoskeleton can be smoothed after extraction, our algorithm is essentially independent of the actual skeletonization algorithm.

Comparing our approach to other vortex core line extraction methods we make the following observations: the algorithm of Stegmaier et al. [SRE05] is a variation of the approach by Banks and Singer [BS95], which constructs a vortex core line from initial seedpoints, following the vorticity vector. It is therefore intrinsically incapable of modeling vortex bifurcations, since the vorticity vector field does not reproduce the bifurcations of the core line. The same holds for the algorithm by Theisel et al. [TSW\*05]. In Section 4 of their paper they model various notions of bifurcation in space-time. However, a model for sole bifurcation in space is not given and can therefore not be detected by their method. Furthermore, the algorithm by Stegmaier et al. may erroneously identify a coherent vortical region as disconnected. Finally, the parallel-vectors approach by Peikert and Roth [PR99] for finding minimal lines is sensitive to noise due to the evaluation of the Hessian (see also Subsection 3.2). Figure 5 compares our approach, the approach of Stegmaier et al., and the parallel-vectors operator for a specific vortex in experimental wake flow behind a cylinder at Reynolds number 540 (measured by tomographic PIV).

To illustrate the effect of the semi-automatic  $\lambda_2$  isovalue determination, we run our algorithm with  $\epsilon$  at 0% and at 5% of the absolute range of  $\lambda_2$  in the dataset. Figure 6 shows that the  $\epsilon$  parameter gives control over the degree of decomposition of vortical regions. While this user-guided solution is a step in the right direction, a fully automated procedure

of isovalue determination would be preferable and could be investigated in future research.

In our approach, the accuracy of the extracted vortex core line is a function of the initial prediction by the isoskeleton. Thus, good results cannot be guaranteed for arbitrarily bad isoskeletons. Figure 6 demonstrates this issue. On the bottom of the right structure a part of the vortex core line cannot be detected due to a missing isoskeleton. Without going into further details of the particular skeletonization approach, we note that skeletonization is still an active field of research and that there is a number of competing approaches (of which very recent work by Hassouna and Farag [HF07] seems promising). Furthermore, provided that a correct and smooth isoskeleton is extracted, the core line prediction and correction process might be iterated in order to improve the accuracy of core line computation (by using the extracted core line as the prediction for the next iteration). While we leave a theoretical proof of convergence as future work, our initial results give reason to believe that such a conjecture is based on solid grounds.

## 7. Conclusion and Future Work

We have introduced a novel  $\lambda_2$ -based vortex core line extraction algorithm that relies on skeletonization of  $\lambda_2$  isosurfaces to guide the construction of the core line. Our approach shows a number of benefits. First, it guarantees the same topology as the curve skeleton. Therefore, the method is robust and can even handle noise-affected data. Second, spatial bifurcation of the vortex core is supported by a model for vortex bifurcations based on connecting core line segments. Third, the determination of the appropriate  $\lambda_2$  isovalue for core line extraction is facilitated in a semi-automatic way through analysis of the topological structure of the  $\lambda_2$  scalar field in order to determine appropriate saddle points at which individual core lines tear. Due to the fact, that the proposed method is a geometric approach, it relies on the quality of the underlying vortex detection criterion. Although we exclusively use the  $\lambda_2$  criterion as basis for vortex core line extraction, any other region-based, local vortex criterion might be applied as long as core lines can be found by searching for local extrema on planes. Future work could investigate the extension of core line extraction to facilitate tracking over

time. Although our current technique with its Galilei invariance allows us to extract core lines of unsteady flow, it provides core lines for each time step independently. Explicit tracking would relate core lines of different times, similarly to previous tracking methods like [BP02, TSW\*05].

## 8. Acknowledgements

We would like to thank Fulvio Scarano (Technische Universiteit Delft) for providing the experimental data set used in Figure 5 and Ulrich Rist (Universität Stuttgart) for the simulated data set used in Figures 3 and 6. Special thanks to Bettina Weiskopf for proof-reading.

## References

- [Adr07] ADRIAN R.: Hairpin vortex organization in wall turbulence. *Physics of Fluids* 19 (2007), 041301.
- [BP02] BAUER D., PEIKERT R.: Vortex tracking in scale-space. In *Proc. EG / IEEE TCVG Symposium on Visualization '02* (2002), pp. 233–240.
- [BS95] BANKS D. C., SINGER B. A.: A predictor-corrector technique for visualizing unsteady flow. *IEEE Transactions on Visualization and Computer Graphics* 1, 2 (1995), 151–163.
- [CM07] CORNEA N. D., MIN P.: Curve-skeleton properties, applications, and algorithms. *IEEE Transactions on Visualization and Computer Graphics* 13, 3 (2007), 530–548.
- [CPC90] CHONG M. S., PERRY A. E., CANTWELL B. J.: A general classification of three-dimensional flow field. *Physics of Fluids A* (1990), 795.
- [CSYB05] CORNEA N. D., SILVER D., YUAN X., BALASUBRAMANIAN R.: Computing hierarchical curve-skeletons of 3D objects. *The Visual Computer* 21, 11 (2005), 945–955.
- [Dal83] DALLMANN U.: *Topological structures of three-dimensional flow separation*. Tech. Rep. DFVLR 221-82-A07, Deutsche Forschungs- und Versuchsanstalt für Luft- und Raumfahrt, 1983.
- [Ebe96] EBERLY D.: *Ridges in Image and Data Analysis. Computational Imaging and Vision*. Kluwer Academic Publishers, 1996.
- [Har83] HARALICK R. M.: Ridges and valleys on digital images. *Computer Vision, Graphics, and Image Processing* 22, 1 (1983), 28–38.
- [HF07] HASSOUNA M. S., FARAG A. A.: On the extraction of curve skeletons using gradient vector flow. *Proc. ICCV 2007* (2007), 1–8.
- [HJ61] HOOKE R., JEEVES T. A.: “Direct search” solution of numerical and statistical problems. *Journal of the ACM* 8, 2 (1961), 212–229.
- [HWM88] HUNT J. C. R., WRAY A. A., MOIN P.: *Eddies, stream, and convergence zones in turbulent flows*. Tech. Rep. CTR-S88, 1988.
- [JH95] JEONG J., HUSSAIN F.: On the identification of a vortex. *Journal of Fluid Mechanics* 285 (1995), 69–94.
- [JMT05] JIANG M., MACHIRAJU R., THOMPSON D.: Detection and visualization of vortices. In *The Visualization Handbook*, Hansen C. D., Johnson C. R., (Eds.). Elsevier, Amsterdam, 2005, pp. 295–309.
- [KT94] KIDA S., TAKAOKA M.: Vortex reconnection. *Annual Review of Fluid Mechanics* 26 (1994), 169–189.
- [LLVT03] LEWINER T., LOPES H., VIEIRA A. W., TAVARES G.: Efficient implementation of Marching Cubes’ cases with topological guarantees. *Journal of Graphics Tools* 8, 2 (2003), 1–15.
- [MK97] MIURA H., KIDA S.: Identification of tubular vortices in turbulence. *Journal of the Physical Society of Japan* 66, 5 (1997), 1331–1334.
- [PR99] PEIKERT R., ROTH M.: The “parallel vectors” operator – a vector field visualization primitive. In *Proc. IEEE Visualization '99* (1999), pp. 263–270.
- [PVH\*03] POST F. H., VROLIJK B., HAUSER H., LARAMEE R. S., DOLEISCH H.: The state of the art in flow visualization: Feature extraction and tracking. *Computer Graphics Forum* 22, 4 (2003), 775–792.
- [SB94] SINGER B. A., BANKS D. C.: *A predictor-corrector scheme for vortex identification*. Tech. Rep. ICASE 94-11, NASA CR-194882, 1994.
- [SH95] SUJUDI D., HAIMES R.: *Identification of swirling flow in 3D vector fields*. Tech. Rep. AIAA 95-1715, Dept. of Aeronautics and Astronautics, MIT, Cambridge, MA, 1995.
- [SRE05] STEGMAIER S., RIST U., ERTL T.: Opening the can of worms: An exploration tool for vortical flows. In *Proc. IEEE Visualization '05* (2005), pp. 463–470.
- [SWH05] SAHNER J., WEINKAUF T., HEGE H.-C.: Galilean invariant extraction and iconic representation of vortex core lines. In *Proc. EG / IEEE VGTC Symposium on Visualization (Eurovis)* (2005), pp. 151–160.
- [TS03] THEISEL H., SEIDEL H.-P.: Feature flow fields. In *Proc. EG / IEEE TCVG Symposium on Visualization '03* (2003), pp. 141–148.
- [TSW\*05] THEISEL H., SAHNER J., WEINKAUF T., HEGE H.-C., SEIDEL H.-P.: Extraction of parallel vector surfaces in 3D time-dependent fields and application to vortex core line tracking. In *Proc. IEEE Visualization '05* (2005), pp. 631–638.
- [vKvOB\*97] VAN KREVELD M., VAN OOSTRUM R., BAJAJ C., PASCUCCI V., SCHIKORE D.: Contour trees and small seed sets for isosurface traversal. In *SCG '97: Proc. Computational Geometry* (1997), pp. 212–220.
- [WSTH07] WEINKAUF T., SAHNER J., THEISEL H., HEGE H.-C.: Cores of swirling particle motion in unsteady flows. *IEEE Transactions on Visualization and Computer Graphics (Proc. Visualization 2007)* 13, 6 (2007), 1759–1766.
- [WXY05] WU J.-Z., XIONG A.-K., YANG Y.-T.: Axial stretching and vortex definition. *Physics of Fluids* 17 (2005), 038108.
- [YOH\*90] YAMADA M., ONO Y., HAYAKAWA A., KATSURAI M., PERKINS F. W.: Magnetic reconnection of plasma toroids with cohelicity and counterhelicity. *Physical Review Letters* 65, 6 (1990), 721–724.